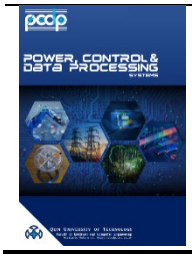
DOI: 10.30511/pcdp.2026.2088672.1072- ISSN: 3060-8376 - Vol 3(4), 2026



POWER, CONTROL AND DATA PROCESSING SYSTEMS

Available Online at: https://pcdp.qut.ac.ir/

Photovoltaic Array Fault Diagnosis Using a semi-supervised method based on Generative Adversarial Networks (GANs)

ARTICLE INFO

Article Type
Original Research

Authors
A. Hadi Almasii[1]
B. Mojtaba Beiraghi[1, *]
C. Reza Ghanizadeh[1]

[1] Department of Electrical Engineering, Ur.C., Islamic Azad University, Urmia, Iran.

**** Correspondence***
Address: Department of electrical and computer engineering, Urmia Branch, Islamic Azad University, Urmia, Iran.
Postal Code: -.
Phone: +989124105574
Fax: -
mojtaba.beiraghi@iau.ac.ir

Article History
Received: May 13, 2026
Accepted: September 10, 2026
ePublished: December 01, 2026

ABSTRACT

Reliable fault diagnosis in photovoltaic (PV) arrays is essential for reducing energy losses, preventing safety hazards, and maintaining system availability; however, conventional supervised learning methods require large labeled datasets that are costly and risky to obtain from operating plants. This paper proposes a data-efficient diagnostic framework that combines convolutional neural networks, semi-supervised generative adversarial learning, and few-shot meta-learning. A 5.3-kW, 6 × 3 PV array is modeled in MATLAB/Simulink to generate healthy and faulty operating data under variations in irradiance, temperature, fault resistance, and partial shading. Four conditions are considered: normal operation, line-to-line faults, hot-spot or high-series-resistance faults, and open-circuit faults. Current, voltage, irradiance, and temperature signals are normalized and transformed using the short-time Fourier transform; their spectrograms are then concatenated into composite images for automatic feature extraction and classification. A three-layer CNN provides a high-accuracy supervised benchmark, reaching approximately 99.5% accuracy on noise-free data. To reduce dependence on labeled samples, a semi-supervised GAN exploits unlabeled and synthetically generated data and achieves 81.57% test accuracy using only 100 labeled samples on the one-dimensional noisy dataset. To further address the computational cost of GAN training and extreme label scarcity, a few-shot meta-learning model is introduced. In the 5-shot, 4-way setting, it achieves 94.03% accuracy on previously unseen samples, substantially outperforming a conventional CNN trained with limited labeled data. The main contribution is therefore a unified comparison of three complementary learning strategies and a practical few-shot solution that preserves strong diagnostic performance with minimal labeled PV fault data under realistic operating variability.

Keywords: Photovoltaic system; Photovoltaic array faults; Fault detection techniques; Semi-supervised learning; Generative adversarial network; Meta learning

1 Introduction

In addressing the growing need for reliable FDD in PV systems, recent research has increasingly turned to advanced machine learning methodologies [1]. Noura et al. demonstrated the efficacy of tree-based algorithms for fault detection and diagnosis in grid-connected photovoltaic systems, crucially incorporating explainable artificial intelligence to render the decision-making processes of these models more transparent and interpretable for operators [1]. Complementing this work on interpretability, Lu et al. tackled the persistent challenge of limited labeled fault data by proposing an efficient fault diagnosis approach that combines a convolutional neural network with a generative adversarial network, showing strong performance in classifying various PV array faults even under small dataset conditions [2]. Beyond algorithmic innovations, the physical configuration of PV arrays themselves has been investigated as a means to enhance fault tolerance; Satpathy et al. conducted an experimental investigation into the electrical fault tolerance of different photovoltaic array configurations, providing valuable performance analysis and monitoring insights that can inform both system design and fault detection strategies [3]. A comprehensive review and performance evaluation of photovoltaic array fault detection and diagnosis techniques was undertaken by Appiah et al., who systematically compared various approaches and established a foundational framework for understanding the strengths and limitations of existing methods [4]. The overarching potential of solar energy as a key component of future sustainable energy systems has been extensively discussed, underscoring the importance of ensuring the reliability of PV installations through effective FDD [5]. Research into the thermal management of solar systems, such as the work by Sun and Wang on heat transfer performance in passive solar collector-storage walls with phase change materials, also highlights the broader context of optimizing solar energy utilization beyond just electrical performance [6]. An online resource for electrical engineers provides supplementary practical knowledge that supports the implementation of monitoring and diagnostic systems in PV installations [7]. Foundational knowledge on PV system modeling and performance prediction has been established to support the optimization of energy yield, which is directly impacted by the presence of faults [8]. Furthermore, the operational dynamics of grid-connected PV systems, particularly regarding the role and performance of grid inverters, have been thoroughly modeled and simulated, providing essential context for understanding how faults in the DC side of the system can affect overall AC power quality and stability [9]. The fundamental principles of solar photovoltaic power generation and system design have been documented, offering a baseline for understanding the operational parameters that FDD systems must monitor [10]. An overview of inverter technologies for single-phase grid-connected systems further details the critical interface between the PV array and the grid, where faults can propagate and cause significant disruptions [11]. Research into the fundamental mechanisms of energy conversion, such as photocarrier generation in organic thin-film solar cells, also contributes to the broader understanding of PV technology and its potential failure modes [12]. Comprehensive texts on advanced renewable energy systems provide the necessary background on system architecture and operational principles that underpin effective FDD strategies [13][14]. Studies on specific power electronics, such as the DC-DC SEPIC converter for maximum power point tracking, have also examined parasitic effects that can influence performance and potentially mimic or exacerbate fault conditions [15]. Furthermore, the ability to pinpoint the exact location and nature of a fault is a significant challenge, with research exploring techniques such as wavelet transforms combined with artificial neural networks to achieve accurate fault location in ungrounded PV systems [16]. These methods, including model-based and signal-based strategies, have been extensively reviewed and form the foundational knowledge base for PV system health monitoring [17]. However, the nonlinear characteristics of PV systems, coupled with the variability of solar irradiance and temperature, often limit the performance and generalizability of these conventional FDD techniques [18]. A detailed analysis of line-line faults in solar photovoltaic arrays has been conducted, highlighting the specific protection challenges and fault characteristics that FDD systems must be designed to address [19]. Additionally, methods for global maximum power point tracking under shading conditions have been developed alongside hotspot detection algorithms, as these conditions are closely related to fault occurrence and can significantly reduce system output [20]. The use of modified particle velocity-based particle swarm optimization for global maximum power point tracking has also been explored, demonstrating the importance of advanced control strategies in mitigating the effects of partial shading, which can often be confused with or lead to permanent faults [21]. This has led to a growing interest in more advanced, data-driven methodologies that can learn complex patterns from operational data and provide more robust and accurate diagnostics [22].

In recent years, the application of machine learning (ML), and particularly deep learning (DL), has revolutionized the field of PV fault detection and diagnosis [22]. A novel CNN-based approach has been specifically developed for fault classification in PV arrays, highlighting the potential of this architecture for robust and automated diagnostics [22]. Beyond CNNs, other deep learning models like autoencoders have been explored for their ability to perform unsupervised anomaly detection, offering a promising path for identifying deviations from normal operational behavior without requiring extensive labeled fault data [23]. The development of these deep learning approaches has been supported by broader advances in the theory and architectures of neural networks, including comprehensive surveys that outline the state-of-the-art in deep learning. Practical guides for implementing deep learning models have also been published, facilitating the

application of these techniques to engineering problems such as PV FDD. Improved CNN architectures, such as those developed for histopathological image classification, have also contributed methodological innovations that can be adapted for analyzing PV data, such as electrical time-series or thermal images. Specific fault types, such as series arc faults in PV systems, have been addressed using novel multi-input neural network architectures, demonstrating the adaptability of deep learning to diverse fault detection challenges. Other machine learning techniques, such as softmax regression models, have been explored for signal classification tasks, offering potential for integration into PV monitoring systems [24].

A persistent challenge in deploying deep learning for PV FDD is the often-limited availability of labeled fault data, which is crucial for training high-performance supervised models. To overcome this data scarcity, the research community is increasingly turning to advanced learning paradigms such as semi-supervised learning and few-shot learning [25-29]. Generative Adversarial Networks have emerged as a powerful tool for semi-supervised learning, where they can generate synthetic, realistic data to augment the limited labeled dataset and simultaneously learn from a larger pool of unlabeled data [30]. The foundational work by Goodfellow et al. on generative adversarial nets has enabled numerous applications in data augmentation and semi-supervised learning [31]. Farajzadeh-Zanjani et al. applied adversarial semi-supervised learning specifically for diagnosing faults and attacks in power grids, demonstrating the practical utility of this approach in related energy systems [32]. Improved techniques for training GANs have also been developed, enhancing their stability and performance for tasks such as data generation for FDD [33]. A survey on implementations of GANs for semi-supervised learning provides a comprehensive overview of the various strategies that can be leveraged for PV FDD when labeled data is scarce [34]. The application of semi-supervised learning using GANs has also been extended to other domains, such as seismic impedance inversion, illustrating the versatility of these methods for problems characterized by limited labeled data [35].Finally, few-shot learning techniques are gaining traction for fault detection in cases where data is extremely limited, offering new ways to enhance fault diagnosis using minimal data [36, 38]. Few-shot learning has shown potential in photovoltaic fault diagnosis by leveraging small amounts of data to train models effectively. This is particularly useful in scenarios where data collection is expensive or time-consuming [39]. Techniques such as meta-learning and prototypical networks have been adapted to improve the performance of fault detection systems in PV arrays, enhancing their ability to generalize from limited examples [40, 44]. Matching networks for one-shot learning offer another approach for classification with extremely limited data, which could be valuable for newly emerging fault types in PV systems [40]. Embedding adaptation methods with set-to-set functions have been developed to further improve few-shot learning by dynamically adjusting feature representations for each task [41]. A comprehensive survey on few-shot learning provides an extensive overview of the field, covering the various methodologies that can be applied to overcome the data scarcity problem in PV fault diagnosis [43]. Prototypical networks have been established as a simple yet effective approach for few-shot learning, computing prototype representations for each class from which new samples can be classified [44]. The use of differentiable Earth Mover's distance for few-shot image classification has also been proposed, offering a robust distance metric for comparing feature distributions [45]. Feature map reconstruction networks have been developed for few-shot classification, learning to reconstruct support set features to classify query samples [46]. Overall, the combination of deep learning, few-shot learning, and advanced neural network architectures has significantly improved the robustness and accuracy of fault diagnosis in photovoltaic arrays, ensuring more reliable and efficient solar power systems [47].

Fault detection in photovoltaic (PV) arrays is crucial due to its role in reducing energy loss and maximizing the revenue from PV systems. It also mitigates the risks and electrical shocks associated with faults in PV arrays. Consequently, a variety of fault detection techniques have been proposed. Since this paper focuses on deep learning-based fault diagnosis methods, we will briefly review several articles related to other fault detection techniques, including comparison-based techniques, statistical and signal processing methods, reflectometry-based techniques, and machine learning approaches. Subsequently, we will provide a more comprehensive review of the literature on fault diagnosis based on deep learning networks. In this category, fault detection and classification are based on comparison values. This comparison can be between the actual measured value of a PV array and the predicted value from its model, between the actual measured values, or between values obtained from the predicted or modeled quantities. It is important to note that the effectiveness and accuracy of a Comparison - Based Techniques (CBT) depend on the quality of the model used for the predicted quantity. A review of articles in this category is presented as follows. In reference [48], faults in photovoltaic arrays, such as short circuits, open circuits, and mismatches, were detected and classified using voltage and current characteristic analysis of the array cells. Figure 1 shows the impact of these faults on the characteristic curves of each array.

Initially, the photovoltaic system model is designed as shown in Figure 2. The presence of a bypass diode for each module is intended to reduce the impact of defective modules on the output current of the modules. The controller then acquires the I-V curves of the arrays and examines them. If the curves differ from those of the main system, the reconfiguration system identifies the location of the fault. For localization, a dual-method approach is introduced. In this method, the author has developed an algorithm that uses functions to detect the type and number of faults in each array. If the number of faults exceeds one, the system divides the array into two sections and repeats the process until each section contains only one fault.

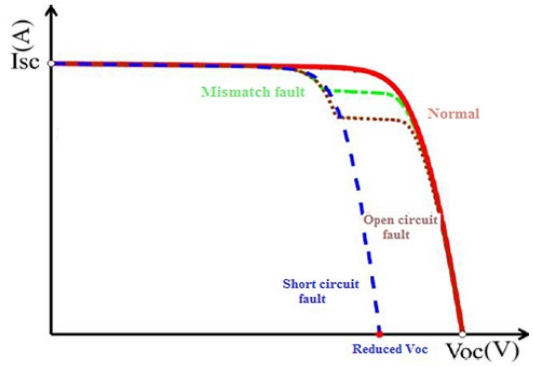


Figure 1: I-V Characteristics of a PV Array for Various Faults.

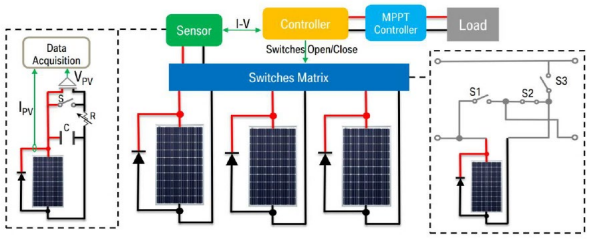


Figure 2: Structure of the Photovoltaic System.

Reference [49] describes a fault detection approach that utilizes comparative analysis between predicted and actual operational data to identify anomalies in photovoltaic (PV) systems without relying on predefined fault models. This technique uses a standard operational framework of the PV setup as a baseline to flag any discrepancies as potential faults. The process is driven by concepts from language theory and employs Petri nets, which are graphical models consisting of places (depicted as circles) and transitions (depicted as rectangles), connected by directed arcs. This setup facilitates the creation of a system-specific language through sequences of operational events, helping in fault identification. In reference [50], the proposed methodology detects faults online by comparing actual measurements to forecasted AC power outputs based on environmental factors like solar irradiance and temperature. This method boasts a detection accuracy over 90% and is favored for its simplicity and cost-efficiency, although it falls short in pinpointing the specific type of fault and its exact location within the PV array. Several researchers have turned to Statistical and Signal Processing-Based Techniques (SSPBTs) to analyze distortions in the output signals of PV systems for fault detection. Reference [51] introduces an online detection method using Wavelet Packet Transform (WPT) and Discrete Wavelet Transform (DWT) to analyze the voltage patterns of PV arrays and identify faults. Yi and Etemadi developed a fault detection method for photovoltaic systems that leverages multi-resolution signal decomposition combined with fuzzy inference systems, demonstrating the effectiveness of integrating signal processing with intelligent decision-making for identifying anomalies [52]. Extending this line of work, the same authors proposed a line-to-line fault detection approach for PV arrays based on multiresolution signal decomposition coupled with a two-stage support vector machine, showcasing the utility of combining advanced signal analysis with powerful classification algorithms [53]. Addressing the specific challenge of series arc faults, Chen and Li introduced a joint detection method that operates effectively under different working conditions, highlighting the importance of robust fault recognition across varying operational scenarios [54]. Mekki et al. explored the use of artificial neural network-based modeling for fault detection of partial shaded photovoltaic modules, demonstrating how neural networks can be trained to recognize the distinctive signatures of shading-induced faults [55]. Alam et al. investigated a fundamentally different approach by applying spread spectrum time domain reflectometry for PV arc-fault detection, illustrating the potential of time-domain reflectometry techniques for identifying faults in PV system wiring [56]. Karatepe and Hiyama developed a control strategy utilizing artificial neural networks for the fault diagnosis of photovoltaic arrays, showcasing early applications of neural networks for this purpose [57]. Garoudja et al. proposed an enhanced machine learning-based approach for failures detection and diagnosis of PV systems, combining multiple techniques to improve diagnostic accuracy [58]. Chen et al. focused on intelligent fault diagnosis using optimized kernel extreme learning machine and I-V characteristics, demonstrating the power of optimized learning algorithms when applied to current-voltage curve data [59]. Further advancing the use of ensemble methods, Chen et al. also developed a random forest based intelligent fault diagnosis approach for PV arrays using array voltage and string currents, achieving robust classification through ensemble learning [60]. Jiang and Maskell proposed an automatic fault detection and diagnosis system that combines artificial neural networks with analytical based methods, leveraging the strengths of both data-driven and model-based approaches [61]. Akram and Lotfifard contributed to the field by developing a method for modeling and health monitoring of the DC side of photovoltaic arrays, providing a framework for continuous health assessment [62]. Finally, Sun et al. applied convolutional neural networks specifically for defect detection of photovoltaic modules, demonstrating the applicability of CNNs for analyzing visual data such as images of PV modules [63].

2 Analyzing Previous Works Based on Deep Learning

The table 1 and 2 provide an overview of the research conducted using deep learning networks, particularly convolutional networks, and then a more detailed examination of several sample studies is provided. PV faults can occur due to a wide range of reasons. Therefore, to prevent irreparable damage to the system, it is essential to develop a robust fault monitoring system. Using data related to the sun's angle, temperature, as well as voltage, current, power, and panel images as inputs for deep learning, the faults and defects that

occur can be detected. These methods overcome the limitations of previous methods and provide higher accuracy in detecting and classifying faults. Most of the existing literature in this field has utilized convolutional neural networks (CNNs) and their derivatives, such as ResNet, LeNet, GoogleNet, and others, for fault diagnosis.

Table 1: overview of references

Year of publication	Model-number of layers	Input	Output	Training data	Test data	Accuracy	Faults
2018 [63]	LetNet-5 6 Layers	Electroluminescent images	4 types of defects and healthy	5120	1000	98.4	Cell leaving, cell exfoliation, outage, broken
2018 [64]	VGG-5 21 Layers	Electroluminescent images	Healthy diagnosis	98280	0	92.3	Cell damage with different levels of broken
2019 [65]	MobileNet 28 Layers	Electroluminescent images	4 types of defects and healthy	28175	18373	89.5	4 figures of hot spot module
2018 [66]	Deep belief network with 4 layers (DBN)	Electroluminescent images	1 type of defects and healthy	200	20	-	Cell braking
2020 [67]	U-net 34 layers	Electroluminescent images	Healthy diagnosis	620	208	100	Cell breakings
2020 [68]	YOLOv3 53 layers	Images available	1 type of defects and healthy	4320	1080	96.3	Pollution (bird droppings, leaves)
2018 [69]	GoogleNet 21 Layers	Electroluminescent images	6 types of defects	720	720	99.7	Crack, hot spot, edge fracture, surface contamination, scratch, area damage
2018 [70]	CNN 9 Layers	Images of the power plant areas	Fault detection and probability	499	88.4	88.4	Defective cell
2019 [71]	ResNet 50 Layers	Images of Modules	Pollution rate	3520	90	90	Pollution (bird droppings, leaves)
2018 [72]	VGG-16 21 Layers	Electroluminescent images	5 types of defects and healthy	2400	90.2	90.2	Encapsulate Delamination, discoloration, glass breakage, contamination, snail marks
2020 [73]	CNN 9 Layers	Electroluminescent images	Healthy diagnosis	-	98.1	98.1	Glass breakage, delamination, pollution, corrosion, snail marks, discoloration
2020 [74]	VGG-16 21 Layers	Images available	1 type of defects and healthy	1372	46.8	46.8	Cell breakings

Table 2: overview of references continued

Year of publication	Model-number of layers	Input	Output	Training data	Test data	Power Plant	Accuracy	Faults
2018 [75]	SAE	Current and voltage time series graph	6 types of defects and healthy	2812	1208	3*4	99/9	Line- -line type, partial shading
2019 [76]	Convolution network 20 Layeres	Current and voltage time series graph	4 types of defects and healthy	981 Test	419 Test	3*6 (1.8KW)	99.5	Line - line, short circuit, 2 types of open circuit
2019 [77]	ResNet 18 Layers	Matrix based on I-V diagram, temperature and radiation	8 types of defects and healthy	15834 simulation and 1870 test	7545 simulation and 897 test	3*6 (1.8KW)	98.1	Open circuit, 3 types of partial shade, 2 types of aging, 2 types of short circuit
2020 [78]	CNN+RNN 6 Layers	Matrix based on I-V diagram, temperature and radiation	9 types of defects and healthy	792 simulation and 1136 test	264 simulation and 377 test	1*13 (3.4KW)	98.4	Open circuit, 3 types of partial shade, 2 types of aging, 2 types of short circuit
2020 [79]	CNN 7 Layers	Matrix extracted from I-V diagram	3 types of defects and healthy	365	90	2*12	99.8	Slight shade, arch flaw, fracture
2020 [22]	AlexNet(transferred) 7 Layers	STFT generated scalogram	5 types of defects and healthy	2419	1037	5*3 (735W)	74.6	Arc defect, line-line, open circuit, 2 types of partial shadows

A comprehensive review and comparison of deep learning models for forecasting electrical energy generation in photovoltaic systems was conducted, with a particular focus on Long Short-Term Memory networks and hybrid models [87]. In parallel, a case study focusing on the modeling and simulation of a solar tracker equipped with bifacial panels was undertaken for the city of Tehran [88]. Furthermore, a separate investigation addressed the broader applicability of deep learning techniques in the renewable energy sector, exploring advanced modeling approaches for photovoltaic systems [89].

3 Proposed Method

3.1 Framework of the Proposed Fault Detection Technique

Figure 3 presents a workflow diagram that delineates the proposed method for detecting faults in PV arrays. The process begins with preprocessing the input data, which is then followed by automatic extraction of features from this data to classify potential faults.

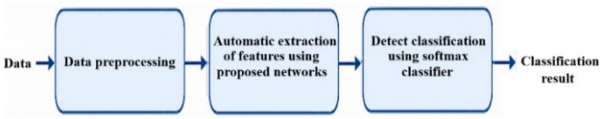


Figure 3: A workflow diagram.

3.2 Data

Deep learning models require extensive datasets to perform optimally. However, assembling such large datasets that include both faulty and normal operational data from a specific PV array is often unfeasible due to factors like unpredictable ambient temperatures and solar irradiance, which cannot be controlled. Moreover, deliberately inducing faults in an actual PV system for data collection could cause significant damage and pose safety risks. Therefore, the data for this study was generated through simulations. Further details on the PV array system model used for data gathering and a comprehensive description of the data collected are outlined below:

3.2.1 Modeling of Photovoltaic Array System

Photovoltaic (PV) cells are commonly modelled using either the single-diode or the double-diode models. The double-diode model, while offering greater accuracy, is less frequently utilized in research due to its complex and non-linear nature, which complicates its ability to precisely depict the current-voltage characteristics of PV cells. In this study, the more widely used single-diode model was employed, facilitated by the MATLAB and Simulink software packages which provide a PV array module based on this model. Using this module, a 5.3 kW PV array system was simulated, as illustrated in Figure 4.

The shading blocks depicted in the Figure 4 above are used to control partial shading levels of the PV array modules.

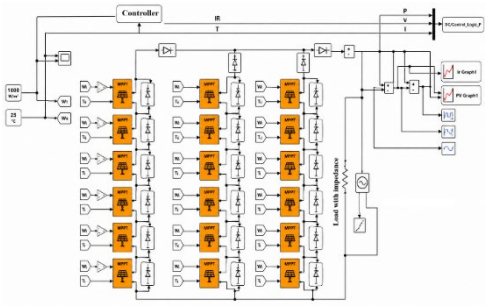


Figure 4: Simulated Solar Power Plant

Table 3 shows the standard test conditions (STC) specifications for the PV module parameters.

Table 3: Specifications of Module Parameters under Standard Conditions.

Items	Parameters	Specification
STC	Temperature	25
	Irradiance	1000
	Maximum power (Pmax)	294.952
PV Module	Voltage at maximum power point (Vmp)	42.8
	Open circuit voltage (Voc)	50.93
	Short circuit current (Isc)	6.2

The model outlined in the previous figure facilitated simulations of both standard and faulty operational states of the PV array for data collection purposes. Figures 5, 6, 7, and 8 display the voltage-current (I-V) characteristics of the PV array under various conditions: no fault, Low-Level Faults (LLF), High Series Resistance Faults (HSF), and Open-Circuit Faults (OCF), respectively.

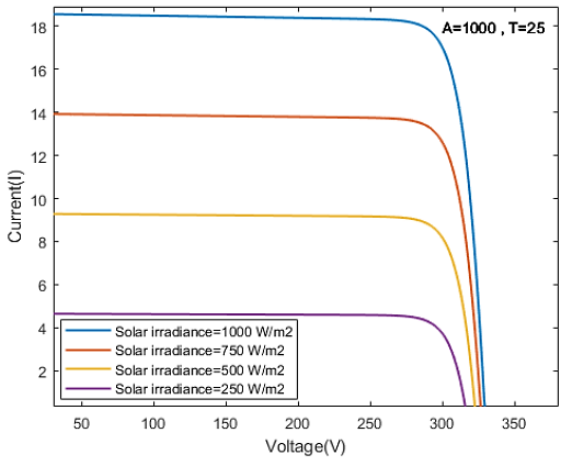


Figure 5: Voltage-Current Characteristics at Different Radiation Levels.

Figure 6 reveals that the output current of the PV array increases with rising solar radiation and decreases as it diminishes, indicating that faults at lower solar radiation levels lead to reduced fault currents. It also shows that, under consistent conditions, the open-circuit voltage of the PV array drops with an increase in mismatch faults, both within strings and between different strings (intra-string and inter-string LLFs), while the short-circuit current remains unchanged. Figure 7 illustrates that partial shading, which results in HSF, distorts the I-V characteristics of the PV array,

creating multiple maximum power points. Lastly, Figure 8 shows that an open-circuit fault causes a decrease in short-circuit current, maintaining nearly constant open-circuit voltage.

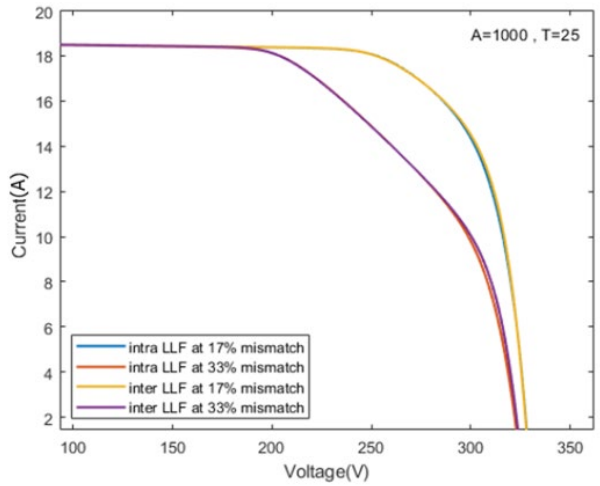


Figure 6: Voltage-Current Characteristics under Line -Line Faults, both Inter- and Intra-String, with Mismatch Percentages of 17% and 30%.

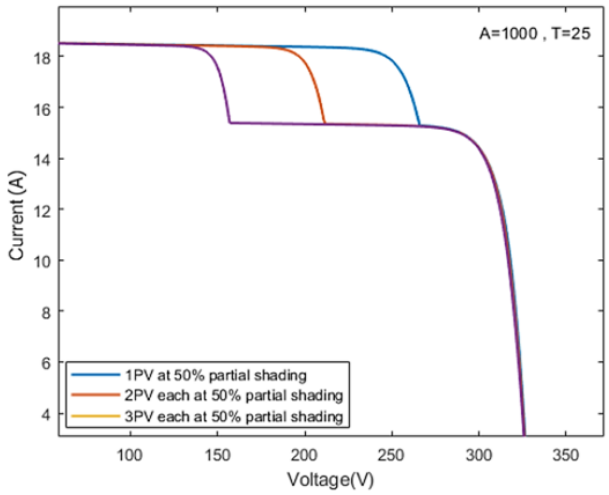


Figure 7: Voltage-Current Characteristics under Hot Spot Fault.

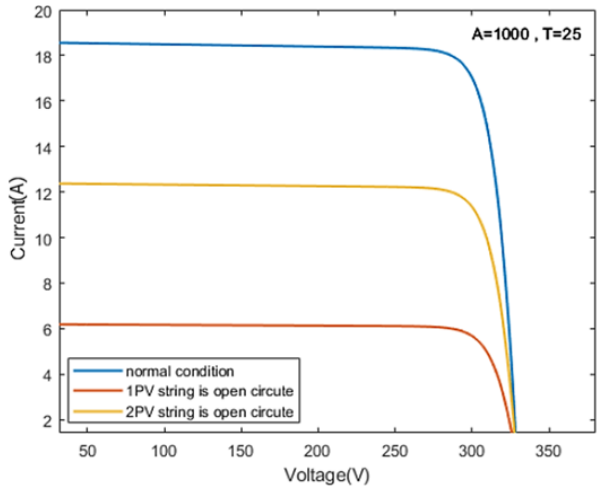


Figure 8: Voltage-Current Characteristics under Open-Circuit Fault.

3.2.2 Data Description

For this study, key variables such as the output current (I), voltage (V), irradiance (G), and temperature (T) of the PV array were recorded. These parameters were chosen for their direct influence on either current or voltage during fault conditions. Data for both fault-free and faulty states was captured, with each state consisting of 1,728 labeled data samples, each sample containing a sequence of 351 data points. The data was generated through simulations that mimicked a variety of real-world conditions, including different combinations of temperatures, irradiance levels, fault impedances, and shading percentages, to ensure realistic and applicable results. Line-Line Fault (LLF): Simulated scenarios included 864 categories with 351 samples each, derived from varying operational temperatures (from 10°C to 50°C in 5°C increments) and irradiance levels (from 50 W/m² to 1200 W/m² in 50 W/m² steps), alongside various fault impedances and mismatch percentages. The simulations were designed to create fault scenarios with low fault current magnitudes that might not be detectable by standard protective devices.

Hot Spot Fault (HSF): For HSF, 432 datasets each containing 351 samples were generated under conditions of 50% partial shading. These simulations varied in temperature and irradiance as described above, to simulate the impact of shading on PV module performance. Open-Circuit Conditions: Data for open-circuit conditions was collected in 216 sets under different temperature and irradiance conditions, reflecting both single and dual-array configurations. Fault-Free Conditions: To compare healthy and faulty states, data was also gathered under fault-free conditions using similar temperature and irradiance ranges, totaling 216 datasets of 351 samples each.

3.2.3 Description of Noisy Data

Although the data in previous section was considered noise-free, real-world data typically contains some level of noise. To mimic these conditions, noise was artificially added to the clean data. This was achieved using the equation:

$$Disturbance = A + B \times randn(1.N) \qquad \text{Eq 1}$$

In this, A represents the mean of the disturbance signal, B denotes the amplitude of the disturbance signal, `randn() ` is a predefined MATLAB noise function, and N is the size of the disturbance signal.

3.2.4 Data Preprocessing

Normalization of Data

Normalization is a critical preprocessing step in both machine learning (ML) and deep learning (DL) algorithms to minimize the impact of variable scales and accelerate algorithm convergence. All data samples were normalized to a range of 0 to 1 and then divided into training, validation, and testing sets, each vectorized into dimensions of 351 for analysis.

Short-Time Fourier Transform (STFT)

To adapt the data for input into the proposed fault detection methods, which require data in image form, the input signals were

transformed into two-dimensional time-frequency spectrograms using the Fourier Transform. The classical Fourier Transform is limited in capturing local signal behaviors; thus, the Short-Time Fourier Transform (STFT) was employed. STFT improves upon the Discrete Fourier Transform (DFT) by allowing for the examination of both instantaneous frequencies and amplitudes, adapting well to the non-stationary nature of photovoltaic signals where characteristics vary over time. This technique involves comparing the signal with basic functions that are localized in both time and frequency, providing a more detailed analysis of the signal's dynamic changes. The SIFT can be driven as:

$$SIFT\{x[n]\} = X(m.\omega) = \sum_{n=-\infty}^{\infty} x[n]\, w[n-m] e^{-j\omega n} \quad \text{Eq 2}$$

where $x[n]$represents the input signal to the transform, sampled at a rate of 360 Hz, and $w[n]$is a window function of finite length. In this proposed method, we use the Hanning Window, which is defined as follows, and the window size is set to 10.

$$w[n] = \begin{cases} 0.5\left[1 - \cos\left(\frac{2\pi n}{M-1}\right)\right] & 0 \le n \le M-1 \\ 0 & otherwise \end{cases} \quad \text{Eq 3}$$

M=10 provides optimal balance, achieving the highest validation accuracy (99.2%) and feature separability (FDR=0.91). Smaller windows (M<10) suffer from poor frequency resolution, failing to distinguish between closely spaced spectral components. Larger windows (M>10) degrade time resolution, losing transient fault signatures.

Therefore, we converted the time-domain signals of the dataset into time-frequency spectrum images. Since we have four input signals, for each signal, we obtained its spectrogram over a specific time interval and then concatenated these four images to form a single composite image. An example of the spectrogram for each category is shown in Figure 9.

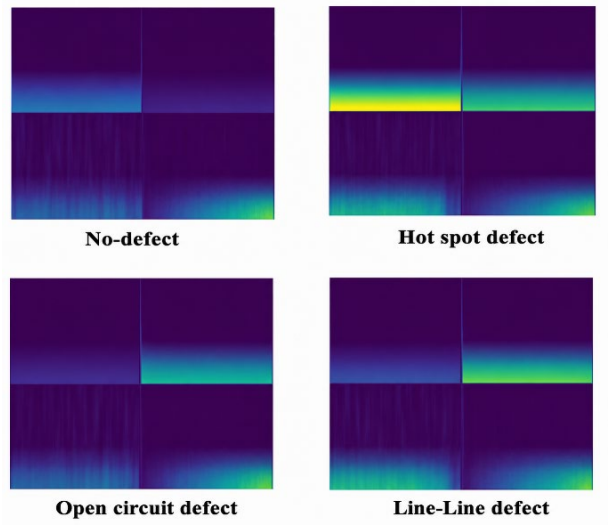


Figure 9: Spectrogram of the data in four different categories

3.3 Proposed Fault Detection Methods

This section introduces three innovative fault detection methods designed to tackle various challenges associated with detecting faults in photovoltaic (PV) arrays. Each method employs different machine learning techniques to optimize performance under varying data conditions.

3.3.1 Convolutional Neural Network

The first proposed method utilizes a Convolutional Neural Network (CNN) to automate the process of feature extraction and fault classification. This CNN comprises three convolutional layers followed by a softmax classifier, a typical setup for image-based classification tasks. Figure 10 depicts the workflow of this approach. The process begins with the preprocessing of data, including normalization and conversion into a two-dimensional format suitable for CNN input. Following preprocessing, the CNN model is trained on a designated training dataset until it reaches convergence. The model's efficacy is then assessed using a separate test dataset to ensure its accuracy and reliability in real-world applications.

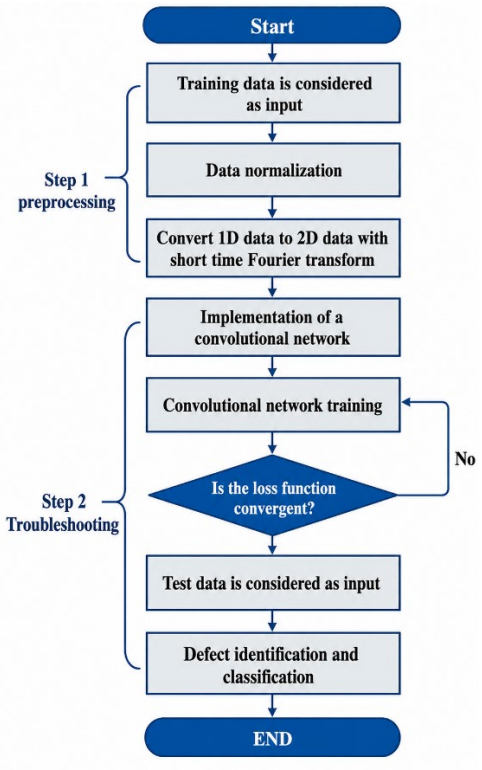


Figure 10: Diagram of the Proposed Approach.

Figure 11 shows a model for the proposed fault detection technique, which controls both automatic feature extraction and fault classification. The CNN and the softmax classifier perform feature extraction and fault classification, respectively. The softmax classifier is designed to have four output nodes.

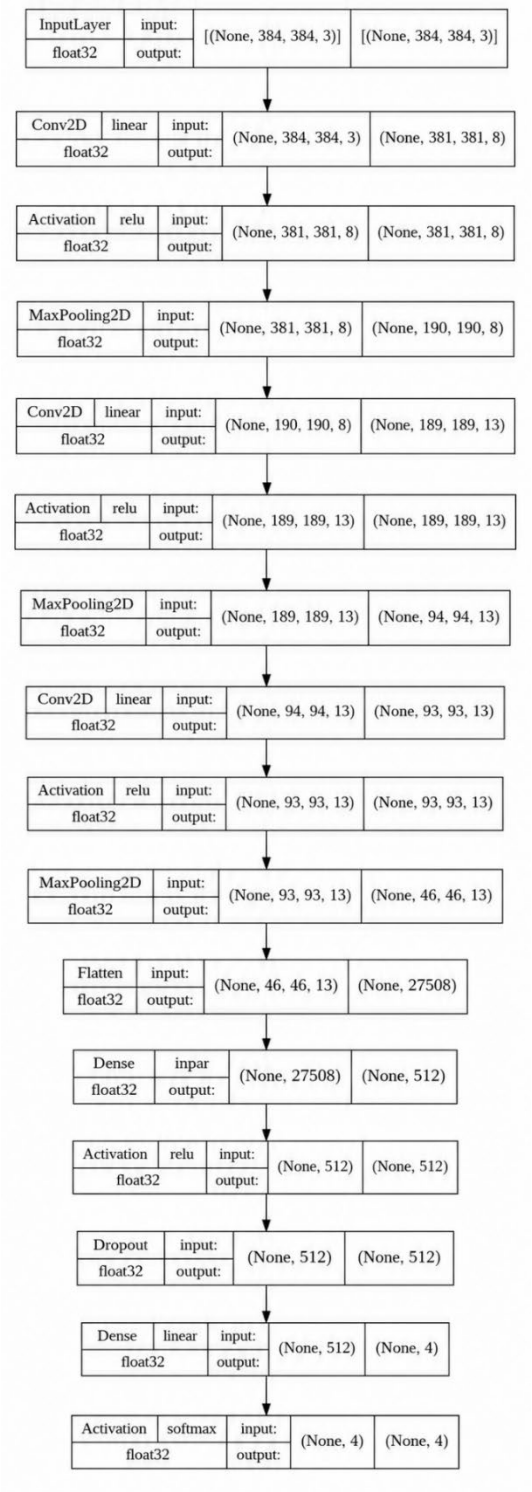


Figure 11: Architecture of the Proposed Network.

4 Results and Analysis

4.1 Experimental Implementation

The evaluation of the proposed fault detection methods was carried out through experimental implementation using the Keras library with TensorFlow as the backend. Keras is a high-level neural networks API written in Python, facilitating the development and execution of deep learning models with its comprehensive suite of tools for building and training neural networks, including optimizers and cost functions.

For the experiments, the noise-free data was divided into training, validation, and testing datasets at a ratio of 10:10:80, respectively. The model was trained and validated using the Keras framework according to the hyper-parameters outlined in Table 4, which were optimized through a grid search method to find the most effective combinations. The performance of the final model was then assessed using the test dataset.

The optimization of the model was performed using the Adaptive Moment Estimation (Adam) algorithm, a method that updates the model's weights and biases based on their computed gradients. Key parameters in this process include the learning rate, which controls how much the parameters change in response to the estimated error each time the model weights are updated, and the batch size, which affects the number of training examples utilized to update the model at each step. An epoch in this context is defined as one complete pass over the entire training dataset.

Table 4: Values of Hyper-Parameters Used in the Network.

Hyper-parameters	value
Batch size	200
Learning rate	0.002
Epoch	600
Node in the FC	256
Node in the softmax layer	4

4.2 Training and Validation Results Based on Noise-Free Data

The training phase was focused on enabling the model to learn the relevant parameters effectively, while validation served to perform error analysis, crucial for identifying potential biases or variance problems. The performance during training and validation was monitored using metrics such as accuracy and loss. Accuracy measures the percentage of predictions that the model got right, while loss provides a quantitative measure of the model's predictions error, helping gauge how closely the output matches the expected results.

Figures 12 and 13 depict the accuracy and loss metrics over the training epochs, demonstrating a steady increase in training accuracy, which peaked at approximately 99.4%. This indicates that the convolutional network and the classification components of the model were effectively learning and optimizing parameters throughout the training process, leading to high levels of accuracy as the model converged to its optimal state. This trend suggests that the model was capable of capturing the underlying patterns in the data, enabling it to predict faults with high reliability in the test scenarios.

As depicted in Figure 12, a consistent and gradual increase in both training and validation accuracy underscores the absence of variance issues within the model, suggesting it is well-primed to generalize effectively to test datasets. An alternative method to gauge training performance, observed through loss plots in Figure

13, reflects that a lower loss at convergence indicates superior model performance. Both training and validation losses approached approximately 0.02 at convergence, underscoring the model's efficacy.

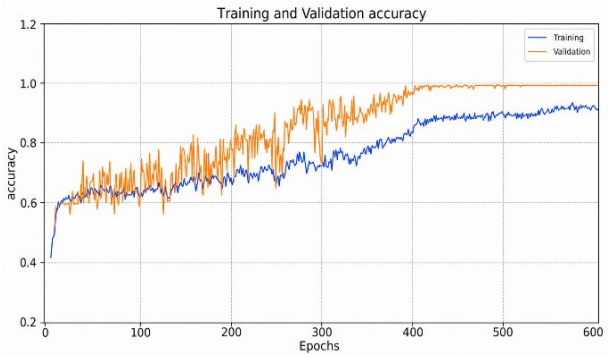


Figure 12: Accuracy Plot for Training and Validation Data.

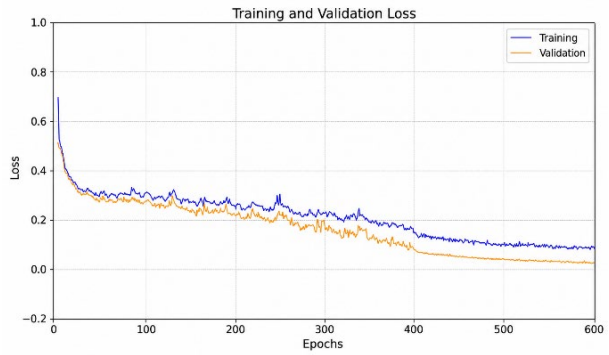


Figure 13: Loss Plot for Training and Validation Data.

4.3 Experimental Results Based on Noise-Free Data

The experimental evaluation involved a multi-class classification for Low-Level Faults (LLF), High Series Resistance Faults (HSF), Open-Circuit Faults (OCF), and Normal Conditions (NC) within the PV array. The classification effectiveness is depicted in a confusion matrix displayed in Figure 14.

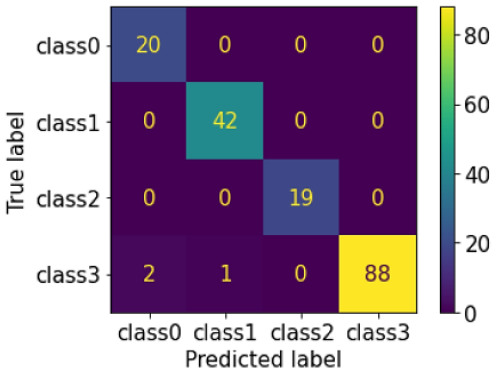


Figure 14: Confusion Matrix.

Each row of the matrix corresponds to the actual classes, and each column reflects the classes predicted by the model. Correct classifications for each type are noted on the matrix diagonal. The model successfully identified 20 samples from class 0 (NC), 42 samples from class 1 (HSF), 19 samples from class 2 (LLF), and 88 samples from class 3 (OCF), with only 3 samples from class 3 misclassified.

The accuracy of classification shows excellent results:

- 100% for Normal Conditions (NC)
- 100% for High Series Resistance Faults (HSF)
- 96.7% for Low-Level Faults (LLF)
- 100% for Open-Circuit Faults (OCF)

These outcomes affirm the model's reliability and its minimal propensity for false fault signals. It also demonstrates strong detection abilities across different fault magnitudes.

4.4 Results of Testing Based on Noisy Data

The gradual degradation in performance with increasing noise levels demonstrates the model's sensitivity to input quality. At low noise levels (10%), performance remains acceptable for practical applications. However, at high noise levels (50%), accuracy drops significantly, highlighting the need for robust denoising preprocessing or more noise-resistant architectures. The SSGAN method showed better noise tolerance (81.6%) compared to the supervised CNN (74.8%), suggesting that the semi-supervised approach learns more robust feature representations. Applying the model to noisy data achieved a detection accuracy of 74.76%. This indicates that although the model has a robust tolerance for noise, extreme noise levels can impair performance. The results, depicted in Fig. 15, suggest that while the model can manage some noise, implementing high-quality sensors is advisable for achieving the best results in real-world settings where noise is common.

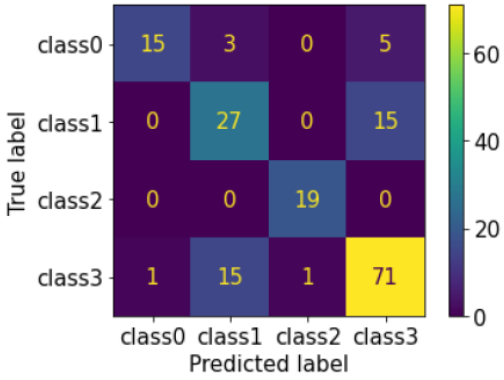


Figure 15: Confusion Matrix for Noisy Data.

4.5 Semi-Supervised Learning with Generative Adversarial Networks

Further tests involved employing a Semi-Supervised Generative Adversarial Network (SSGAN) for fault detection, using the same 100 labeled samples initially used for the CNN training. The SSGAN notably enhanced the classification accuracy, underscoring the benefits of incorporating unlabeled data to improve the model's efficacy.

Fig. 16 illustrates the SSGAN's structure, featuring generator and discriminator networks. This structure is further elaborated in subsequent sections to clarify each component's role in bolstering the model's overall effectiveness and addressing the challenges associated with limited labeled data. This method shows potential for advancing fault detection capabilities in PV systems through sophisticated machine learning strategies.

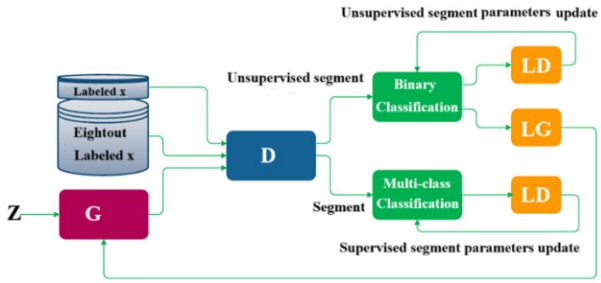


Figure 16: The Architecture of a Semi-Supervised Learning Network Based on Generative Adversarial Networks (GANs).

4.6 Generator Model

The generator's architecture is depicted in Figure 17. It utilizes transposed convolutional layers to create an image from random noise, incorporating three such layers to achieve the target image dimensions.

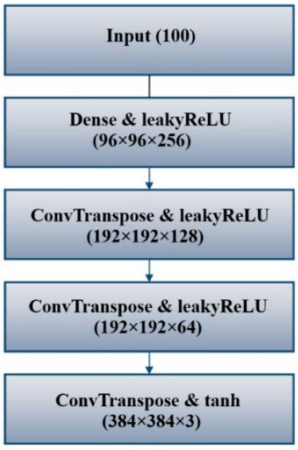


Figure 17: The Architecture of the Generator Network.

Each layer is followed by a Leaky Rectified Linear Unit (LeakyReLU) activation function, except for the final output layer, which employs a tanh activation function. The network maintains data dimensions consistently across all layers by using zero-padding in its convolutions. It also uses Rectified Linear Unit (ReLU) as the activation function and includes Batch Normalization (BN) to expedite the network's convergence, as noted in [86].

4.7 Generator Model

Conversely, the discriminator's role is to differentiate between the frequency-time spectrums produced by the generator and actual spectrums. Inputs to the discriminator include spectrums generated by the generator, along with unlabeled real images and 100 labeled images, distributed evenly across four categories (25 images from each category). As illustrated in Figure 18, the discriminator's architecture mirrors that of the generator, featuring three convolutional layers activated by leaky ReLU, culminating in a softmax classifier for categorization.

This model uniquely integrates both supervised and unsupervised learning components. Rather than maintaining two distinct models, a novel strategy introduced in [33] incorporates an additional layer preceding the softmax activator to generate an unsupervised output. This unsupervised component assimilates outputs from the supervised section, as shown just before the softmax layer. It computes the normalized sum of the exponential outputs according to an equation from [33], effectively classifying images as either fake or real.

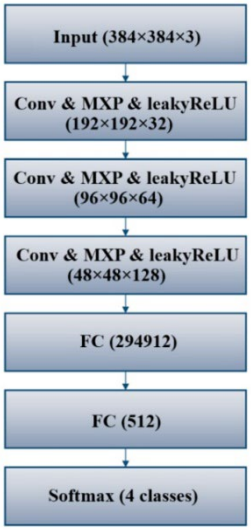


Figure 18: The Architecture of the Discriminator Network

$$x(x) = \sum_{k=1}^{k} \exp[L_k(x)] \qquad D(x) = \frac{z(x)}{z(x)+1} \qquad \text{Eq 4}$$

The SSGAN network is trained similarly to the GAN network, except for the supervised part. Initially, the weights of the supervised section are updated using the labels and the loss of the supervised section. Then, the unsupervised section is updated according to the unsupervised discriminator loss using unlabeled and fake data. Finally, the generator's weights are updated based on the generator loss, as described in Section 2.

An example of a fake image generated by the generator network for each category is shown in Fig. 19. It can be observed that distinguishing these generated images from real images is extremely difficult, if not impossible, for a human. Therefore, the discriminator network must be very powerful to differentiate these images, and the generator network should be updated at each stage to produce more realistic images. It should be noted that this generated image was created with only 20 training epochs due to the lack of a powerful system. This network, due to generating images, requires a high-performance graphics card and GPU. Thus, all the results of this technique were achieved with only 20 epochs, and we have obtained very good results compared to

related studies, which typically involve training and updating parameters for up to 5000 epochs.

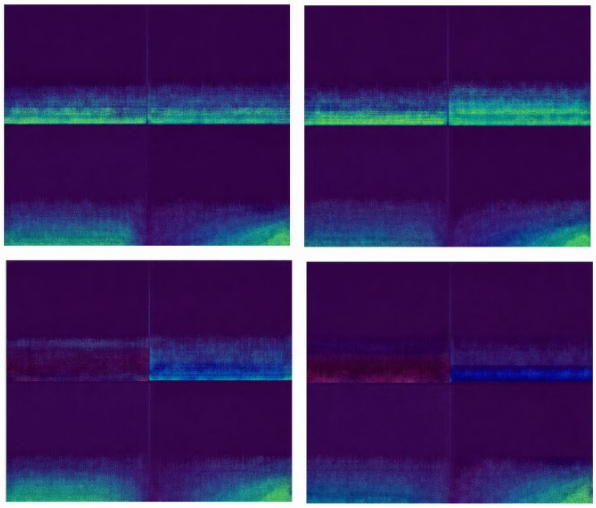


Figure 19: An Example of Generated Images from Each Category by the GAN Network.

The Adam optimization algorithm (Adaptive Moment Estimation) was used with a learning rate of 0.0001 and a batch size of 100. The network was trained for 20 epochs. The proposed network was evaluated using 344 test data samples, achieving an accuracy of 60% on noisy data. Figure 20 presents the results obtained on the noisy data.

To validate the presented concepts, this method was tested with one-dimensional data, which requires less memory and does not demand a large volume of fake data generation. The network used in this section is similar to the network described for image data, except that one-dimensional convolution is used in the architecture of the generator and discriminator. The results were obtained after 500 epochs with a learning rate of 0.0002. The training accuracy was 91.55%, and the test accuracy was 81.57%.

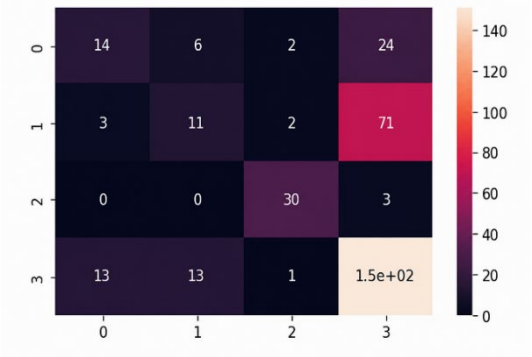


Figure 20: Confusion Matrix.

The training of the GAN model required significant computational resources, with training time averaging 48 hours on a high-performance GPU. Inference time was 0.35 seconds per sample on the same hardware. The memory requirement for training the model was approximately 8 GB of GPU memory. These results indicate that the model can be deployed in real-time PV monitoring systems with adequate hardware.

4.8 Learning from Limited Data with Initial Networks

As demonstrated, we initially trained a network using 1,384 labeled data samples. The evaluation accuracy achieved with 344 test data samples was approximately 59.9%. Subsequently, using the semi-supervised learning method based on GAN networks, we trained a network with only 100 labeled data samples and a large number of unlabeled data samples. After only 20 epochs, we achieved an evaluation accuracy of 60% for image data. In this section, a new approach in the context of learning is employed, where we managed to achieve an evaluation accuracy of 94% with only 5 labeled samples from each category and 8 query samples in each Episode.

This method consists of two parts: meta-training and meta-testing. In the meta-testing phase, a 4-layer convolutional network with 64 filters is used. For training this network, 200 image samples are used as input, which can be entirely different from our own data; for example, here, the ImageNet dataset is used. The training of the network is entirely different from classical deep learning networks; thus, the data is not fed into the network all at once. Instead, in each episode, batches of 5 images from 4 different categories are used for training, and the training is evaluated with 8 query samples. The architecture of this convolutional network is shown in Figure. 21.

In the second phase, known as meta-testing, we used 76 data samples for evaluation. In each episode, a support set consisting of 5 samples from each category and a query set consisting of 8 samples were utilized. These data samples were entirely different from those used in meta-training. In the Few-Shot learning context, our 5-Shot-4-Way problem achieved a classification accuracy of 94% on completely new and unseen data. In this section, a novel approach in the context of meta-learning is employed, where we achieved an evaluation accuracy of 94.03% with only 5 labeled samples from each category and 8 query samples in each episode. This method consists of two parts: meta-training and meta-testing. In the meta-training phase, a 4-layer convolutional network with 64 filters is used. For training this network, 200 image samples are used as input, which can be entirely different from our own data. The training is entirely different from classical deep learning networks; data is not fed into the network all at once. Instead, in each episode, batches of 5 images from 4 different categories are used for training, and the training is evaluated with 8 query samples.

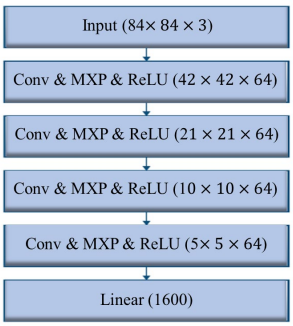


Figure 21: Architecture of the FSL Network

We also investigated the problem with 10-Shot-4-Way, 10-Shot-2-Way, and 5-Shot-2-Way scenarios, and the results obtained are presented in the table 5.

Table 5: Comparison of Results.

Number of images-Number of batches	Accuracy of Evaluation
5Shot-4way	94.03
5Shot-2way	97.43
10Shot-4way	95.37
10Shot-2way	98.12

As observed from the table, the test accuracy with two categories is higher than with four categories. In each case, two categories are selected randomly for evaluation. This finding can be utilized in future research to systematically analyze pairs of categories in a tree-like structure.

5 Conclusion

The data used for fault detection in PV arrays in various studies were labeled. However, collecting labeled data in the industry is highly costly and challenging due to the need for defect identification and subsequent collection of data resulting from those defects. In some cases, this process can even lead to fires and damage to panels in solar power plants. To address these challenges, a semi-supervised method based on Generative Adversarial Networks (GANs) was introduced in this research. Voltage, current, temperature, and radiation were considered as input data and collected from a 6×3 simulated power plant in Simulink. Since the Backbone methodology employed in this paper involved Convolutional Neural Networks (CNNs), we required two-dimensional data as input. To this end, we used the Short-Time Fourier Transform to convert one-dimensional data into two-dimensional spectrograms. Initially, with 1,728 data sets and a three-layer convolutional network, we achieved a classification accuracy of 99.5% for defect identification. To address the issue of data scarcity, we employed a GAN-based semi-supervised learning approach and performed defect diagnosis with only 100 labeled data samples. The results showed that this method could classify defects with an accuracy of 81.57%. While the proposed method addressed the challenge of data scarcity, the storage of generated images by the GAN network and the large volume of images necessitated a powerful system with a high-performance graphics card for network training. Due to the lack of access to such a system, we also introduced a supplementary technique (few-shot learning). This technique achieved a classification accuracy of 95% with only 5 labeled samples. We compared the proposed methods with a CNN network trained with only 200 labeled data samples, which achieved an evaluation accuracy of 30%. Thus, the superiority of the proposed methods over the supervised approaches mentioned in the literature is clearly demonstrated. Future improvements include testing the model in real-time PV systems, enhancing noise robustness, and exploring the scalability of the approach for large PV plants.

Potential Conflicts of Interest

The Authors declare that there is no conflict of interest

Reference

[1] Noura, Hassan N., Zaid Allal, Ola Salman, and Khaled Chahine. "Explainable artificial intelligence of tree-based algorithms for fault detection and diagnosis in grid-connected photovoltaic systems." Engineering Applications of Artificial Intelligence 139 (2025): 109503. DOI: https://doi.org/10.1016/j.engappai.2024.109503

[2] Lu, Xiaoyang, Yaohai Lin, Peijie Lin, Xiangjian He, Gengfa Fang, Shuying Cheng, Zhicong Chen, and Lijun Wu. "Efficient fault diagnosis approach for solar photovoltaic array using a convolutional neural network in combination of generative adversarial network under small dataset." Solar Energy 253 (2023): 360-374. DOI: https://doi.org/10.1016/j.solener.2022.12.037

[3] Satpathy, Priya Ranjan, Belqasem Aljafari, Sudhakar Babu Thanikanti, and Siva Rama Krishna Madeti. "Electrical fault tolerance of photovoltaic array configurations: Experimental investigation, performance analysis, monitoring and detection." Renewable Energy 206 (2023): 960-981. DOI: https://doi.org/10.1016/j.renene.2023.02.103

[4] A. Y. Appiah, X. Zhang, B. B. K. Ayawli, and F. Kyeremeh, "Review and performance evaluation of photovoltaic array fault detection and diagnosis techniques," Int. J. Photoenergy, vol. 2019, 2019. DOI: https://doi.org/10.1155/2019/6953530

[5] E. Kabir, P. Kumar, S. Kumar, A. A. Adelodun, and K.-H. Kim, "Solar energy: Potential and future prospects," Renew. Sustain. Energy Rev., vol. 82, pp. 894–900, 2018. DOI: https://doi.org/10.1016/j.rser.2017.09.094

[6] D. Sun and L. Wang, "Research on heat transfer performance of passive solar collector-storage wall system with phase change materials," Energy Build., vol. 119, pp. 183–188, 2016. DOI: https://doi.org/10.1016/j.enbuild.2016.03.048

[7] "Electrical Engineering 123 – Resources For Electrical & Electronic Engineers." https://electricalengineering123.com/ (accessed Sep. 07, 2020). DOI: Not available.

[8] T. Ma, H. Yang, and L. Lu, "Solar photovoltaic system modeling and performance prediction," Renewable and Sustainable Energy Reviews, vol. 36. pp. 304–315, 2014. DOI: https://doi.org/10.1016/j.rser.2014.04.057

[9] A. M. Bin Omar and H. binti Zainuddin, "Modeling and simulation of grid inverter in grid-connected photovoltaic system," Int. J. Renew. Energy Res., vol. 4, no. 4, pp. 949–957, 2014. Alternative DOI (journal issue): https://doi.org/10.20508/ijrer.v4i4

[10] S. Shaari, A. M. Omar, A. H. Haris, and S. I. Sulaiman, "Solar photovoltaic power: Fundamentals," Putrajaya Minist. Energy, Green Technol. Water, 2010. DOI: Not available.

[11] M. Calais, J. Myrzik, T. Spooner, and V. G. Agelidis, "Inverters for single-phase grid connected photovoltaic systems-an overview," in 2002 IEEE 33rd Annual IEEE Power Electronics Specialists Conference. Proceedings (Cat. No. 02CH37289), 2002, vol. 4, pp. 1995–2000. DOI: https://doi.org/10.1109/PSEC.2002.1023107

[12] T. Osasa, S. Yamamoto, Y. Iwasaki, and M. Matsumura, "Photocarrier generation in organic thin-film solar cells with an organic heterojunction," Sol. energy Mater. Sol. cells, vol. 90, no. 10, pp. 1519–1526, 2006. DOI: https://doi.org/10.1016/j.solmat.2005.10.016

[13] S. C. Bhatia, Advanced renewable energy systems,(Part 1 and 2). CRC Press, 2014. DOI: Not available.

[14] M. H. Rashid, Power electronics handbook: devices, circuits and applications. Elsevier, 2010. DOI: Not available.

[15] N. Mohammad, M. Quamruzzaman, M. R. T. Hossain, and M. R. Alam, "Parasitic effects on the performance of dc-dc sepic in photovoltaic maximum power point tracking applications," 2013. DOI: https://doi.org/10.4236/sgre.2013.41014

[16] I. M. Karmacharya and R. Gokaraju, "Fault location in ungrounded photovoltaic system using wavelets and ANN," IEEE Trans. Power Deliv., vol. 33, no. 2, pp. 549–559, 2017. DOI: https://doi.org/10.1109/TPWRD.2017.2721903

[17] A. Y. Appiah, X. Zhang, B. B. K. Ayawli, and F. Kyeremeh, "Review and performance evaluation of photovoltaic array fault detection and diagnosis techniques," Int. J. Photoenergy, vol. 2019, 2019. DOI: https://doi.org/10.1155/2019/6953530

[18] Y.-Y. Hong and R. A. Pula, "Detection and classification of faults in photovoltaic arrays using a 3D convolutional neural network," Energy, vol. 246, p. 123391, 2022. DOI: https://doi.org/10.1016/j.energy.2022.123391

[19] Y. Zhao, J.-F. De Palma, J. Mosesian, R. Lyons, and B. Lehman, "Line–line fault analysis and protection challenges in solar photovoltaic arrays," IEEE Trans. Ind. Electron., vol. 60, no. 9, pp. 3784–3795, 2012. DOI: https://doi.org/10.1109/TIE.2012.2205355

[20] J. Gosumbonggot and G. Fujita, "Global maximum power point tracking under shading condition and hotspot detection algorithms for photovoltaic systems," Energies, vol. 12, no. 5, p. 882, 2019. DOI: https://doi.org/10.3390/en12050882

[21] T. Sen, N. Pragallapati, V. Agarwal, and R. Kumar, "Global maximum power point tracking of PV arrays under partial shading conditions using a modified particle velocity-based PSO technique," IET Renew. Power Gener., vol. 12, no. 5, pp. 555–564, 2018. DOI: https://doi.org/10.1049/iet-rpg.2016.0838

[22] F. Aziz, A. Ul Haq, S. Ahmad, Y. Mahmoud, M. Jalal, and U. Ali, "A Novel Convolutional Neural Network-Based Approach for Fault Classification in Photovoltaic Arrays," IEEE Access, vol. 8. pp. 41889–41904, 2020. DOI: https://doi.org/10.1109/ACCESS.2020.2977116

[23] Seghiour, Abdellatif, Hamou Ait Abbas, Aissa Chouder, and Abdlhamid Rabhi. "Deep learning method based on autoencoder neural network applied to faults detection and diagnosis of photovoltaic system." Simulation Modelling Practice and Theory 123 (2023): 102704. DOI: https://doi.org/10.1016/j.simpat.2022.102704

[24] V. Venkatasubramanian, R. Rengaswamy, K. Yin, and S. N. Kavuri, "A review of process fault detection and diagnosis part I: Quantitative model-based methods," Comput. Chem. Eng., vol. 27, no. 3, pp. 293–311, 2003. DOI: https://doi.org/10.1016/S0098-1354(02)00160-6

[25] M. Z. Alom et al., "A state-of-the-art survey on deep learning theory and architectures," Electronics, vol. 8, no. 3, p. 292, 2019. DOI: https://doi.org/10.3390/electronics8030292

[26] J. Patterson and A. Gibson, Deep learning: A practitioner's approach. " O'Reilly Media, Inc.," 2017. DOI: Not available.

[27] A. Gulli and S. Pal, Deep learning with Keras. Packt Publishing Ltd, 2017. DOI: Not available.

[28] V. Rachapudi and G. L. Devi, "Improved convolutional neural network based histopathological image classification," Evol. Intell., pp. 1–7, 2020. DOI: https://doi.org/10.1007/s12065-020-00367-y

[29] X. Chen, W. Gao, C. Hong, and Y. Tu, "A novel series arc fault detection method for photovoltaic system based on multi-input neural network," Int. J. Electr. Power Energy Syst., vol. 140, p. 108018, 2022. DOI: https://doi.org/10.1016/j.ijepes.2022.108018

[30] L. Zhang, H. Huang, and X. Jing, "A modified cyclostationary spectrum sensing based on softmax regression model," in 2016 16th International Symposium on Communications and Information Technologies (ISCIT), 2016, pp. 620–623. DOI: https://doi.org/10.1109/ISCIT.2016.7751707

[31] I. Goodfellow et al., "Generative adversarial nets," Adv. Neural Inf. Process. Syst., vol. 27, 2014. Alternative DOI (arXiv): https://doi.org/10.48550/arXiv.1406.2661

[32] M. Farajzadeh-Zanjani, E. Hallaji, R. Razavi-Far, M. Saif, and M. Parvania, "Adversarial semi-supervised learning for diagnosing faults and attacks in power grids," IEEE Trans. Smart Grid, vol. 12, no. 4, pp. 3468–3478, 2021. DOI: https://doi.org/10.1109/TSG.2021.3061395

[33] T. Salimans, I. Goodfellow, W. Zaremba, V. Cheung, A. Radford, and X. Chen, "Improved techniques for training gans," Adv. Neural Inf. Process. Syst., vol. 29, 2016. Alternative DOI (arXiv): https://doi.org/10.48550/arXiv.1606.03498

[34] A. R. Sajun and I. Zualkernan, "Survey on Implementations of Generative Adversarial Networks for Semi-Supervised Learning," Appl. Sci., vol. 12, no. 3, p. 1718, 2022. DOI: https://doi.org/10.3390/app12031718

[35] B. Wu, D. Meng, and H. Zhao, "Semi-supervised learning for seismic impedance inversion using generative adversarial networks," Remote Sens., vol. 13, no. 5, p. 909, 2021. DOI: https://doi.org/10.3390/rs13050909

[36] F. Sung, Y. Yang, L. Zhang, T. Xiang, P. H. S. Torr, and T. M. Hospedales, "Learning to compare: Relation network for few-shot learning," in Proceedings of the IEEE conference on computer vision and pattern recognition, 2018, pp. 1199–1208. DOI: https://doi.org/10.1109/CVPR.2018.00131

[37] S. Yang, L. Liu, and M. Xu, "Free lunch for few-shot learning: Distribution calibration," arXiv Prepr. arXiv2101.06395, 2021. Alternative DOI (arXiv): https://doi.org/10.48550/arXiv.2101.06395

[38] Z. Ji, X. Chai, Y. Yu, Y. Pang, and Z. Zhang, "Improved prototypical networks for few-Shot learning," Pattern Recognit. Lett., vol. 140, pp. 81–87, 2020. DOI: https://doi.org/10.1016/j.patrec.2020.07.015

[39] A. Santoro, S. Bartunov, M. Botvinick, D. Wierstra, and T. Lillicrap, "Meta-learning with memory-augmented neural networks," in International conference on machine learning, 2016, pp. 1842–1850. Alternative DOI (arXiv): https://doi.org/10.48550/arXiv.1605.06065

[40] O. Vinyals, C. Blundell, T. Lillicrap, and D. Wierstra, "Matching networks for one shot learning," Adv. Neural Inf. Process. Syst., vol. 29, 2016. Alternative DOI (arXiv): https://doi.org/10.48550/arXiv.1606.04080

[41] H.-J. Ye, H. Hu, D.-C. Zhan, and F. Sha, "Few-shot learning via embedding adaptation with set-to-set functions," in Proceedings of the IEEE/CVF Conference on Computer Vision and Pattern Recognition, 2020, pp. 8808–8817. DOI: https://doi.org/10.1109/CVPR42600.2020.00883

[42] K. Lee, S. Maji, A. Ravichandran, and S. Soatto, "Meta-learning with differentiable convex optimization," in Proceedings of the IEEE/CVF Conference on Computer Vision and Pattern Recognition, 2019, pp. 10657–10665. DOI: https://doi.org/10.1109/CVPR.2019.01091

[43] Y. Wang, Q. Yao, J. T. Kwok, and L. M. Ni, "Generalizing from a few examples: A survey on few-shot learning," ACM Comput. Surv., vol. 53, no. 3, pp. 1–34, 2020. DOI: https://doi.org/10.1145/3386252

[44] J. Snell, K. Swersky, and R. Zemel, "Prototypical networks for few-shot learning," Adv. Neural Inf. Process. Syst., vol. 30, 2017. DOI : https://doi.org/10.48550/arXiv.1703.05175

[45] C. Zhang, Y. Cai, G. Lin, and C. Shen, "Deepemd: Few-shot image classification with differentiable earth mover's distance and

structured classifiers," in Proceedings of the IEEE/CVF conference on computer vision and pattern recognition, 2020, pp. 12203–12213. DOI: https://doi.org/10.1109/CVPR42600.2020.01222

[46] D. Wertheimer, L. Tang, and B. Hariharan, "Few-shot classification with feature map reconstruction networks," in Proceedings of the IEEE/CVF Conference on Computer Vision and Pattern Recognition, 2021, pp. 8012–8021. DOI: https://doi.org/10.1109/CVPR46437.2021.00792

[47] M. Al-Shedivat, L. Li, E. Xing, and A. Talwalkar, "On data efficiency of meta-learning," in International Conference on Artificial Intelligence and Statistics, 2021, pp. 1369–1377. DOI (arXiv): https://doi.org/10.48550/arXiv.2102.00127

[48] D. Ji, C. Zhang, M. Lv, Y. Ma, and N. Guan, "Photovoltaic array fault detection by automatic reconfiguration," Energies, vol. 10, no. 5. 2017. DOI: https://doi.org/10.3390/en10050699

[49] M. Muñoz, A. Correcher, E. Ariza, E. García, and F. Ibañez, "Fault detection and isolation in a photovoltaic system," Renewable Energy and Power Quality Journal, vol. 1, no. 13. pp. 202–207, 2015. DOI: https://doi.org/10.24084/repqj13.281

[50] R. Platon, J. Martel, N. Woodruff, and T. Y. Chau, "Online fault detection in PV systems," IEEE Trans. Sustain. Energy, vol. 6, no. 4, pp. 1200–1207, 2015. DOI: https://doi.org/10.1109/TSTE.2015.2421447

[51] B. P. Kumar, G. S. Ilango, M. J. B. Reddy, and N. Chilakapati, "Online fault detection and diagnosis in photovoltaic systems using wavelet packets," IEEE J. Photovoltaics, vol. 8, no. 1, pp. 257–265, 2017. DOI: https://doi.org/10.1109/JPHOTOV.2017.2770159

[52] Z. Yi and A. H. Etemadi, "Fault detection for photovoltaic systems based on multi-resolution signal decomposition and fuzzy inference systems," IEEE Trans. Smart Grid, vol. 8, no. 3, pp. 1274–1283, 2016. DOI: https://doi.org/10.1109/TSG.2016.2587244

[53] Z. Yi and A. H. Etemadi, "Line-to-line fault detection for photovoltaic arrays based on multiresolution signal decomposition and two-stage support vector machine," IEEE Trans. Ind. Electron., vol. 64, no. 11, pp. 8546–8556, 2017. DOI: https://doi.org/10.1109/TIE.2017.2703681

[54] S. Chen and X. Li, "PV series arc fault recognition under different working conditions with joint detection method," in 2016 IEEE 62nd Holm Conference on Electrical Contacts (Holm), 2016, pp. 25–32. DOI: https://doi.org/10.1109/HOLM.2016.7780002

[55] H. Mekki, A. Mellit, and H. Salhi, "Artificial neural network-based modelling and fault detection of partial shaded photovoltaic modules," Simul. Model. Pract. Theory, vol. 67, pp. 1–13, 2016. DOI: https://doi.org/10.1016/j.simpat.2016.05.005

[56] M. K. Alam, F. H. Khan, J. Johnson, and J. Flicker, "PV arc-fault detection using spread spectrum time domain reflectometry (SSTDR)," in 2014 IEEE energy conversion congress and exposition (ECCE), 2014, pp. 3294–3300. DOI: https://doi.org/10.1109/ECCE.2014.6953848

[57] E. Karatepe and T. Hiyama, "Controlling of artificial neural network for fault diagnosis of photovoltaic array," in 2011 16th International Conference on Intelligent System Applications to Power Systems, 2011, pp. 1–6. DOI: https://doi.org/10.1109/ISAP.2011.6082219

[58] E. Garoudja, A. Chouder, K. Kara, and S. Silvestre, "An enhanced machine learning based approach for failures detection and diagnosis of PV systems," Energy Convers. Manag., vol. 151, pp. 496–513, 2017. DOI: https://doi.org/10.1016/j.enconman.2017.09.019

[59] Z. Chen, L. Wu, S. Cheng, P. Lin, Y. Wu, and W. Lin, "Intelligent fault diagnosis of photovoltaic arrays based on optimized kernel extreme learning machine and IV characteristics," Appl. Energy, vol. 204, pp. 912–931, 2017. DOI: https://doi.org/10.1016/j.apenergy.2017.05.034

[60] Z. Chen et al., "Random forest based intelligent fault diagnosis for PV arrays using array voltage and string currents," Energy Convers. Manag., vol. 178, pp. 250–264, 2018. DOI: https://doi.org/10.1016/j.enconman.2018.10.040

[61] L. L. Jiang and D. L. Maskell, "Automatic fault detection and diagnosis for photovoltaic systems using combined artificial neural network and analytical based methods," in 2015 International Joint Conference on Neural Networks (IJCNN), 2015, pp. 1–8. DOI: https://doi.org/10.1109/IJCNN.2015.7280498

[62] M. N. Akram and S. Lotfifard, "Modeling and health monitoring of DC side of photovoltaic array," IEEE Trans. Sustain. Energy, vol. 6, no. 4, pp. 1245–1253, 2015. DOI: https://doi.org/10.1109/TSTE.2015.2425791

[63] M. Sun, S. Lv, X. Zhao, R. Li, W. Zhang, and X. Zhang, "Defect detection of photovoltaic modules based on convolutional neural network," in International Conference on Machine Learning and Intelligent Communications, 2017, pp. 122–132. DOI: https://doi.org/10.1007/978-3-319-73564-1_13

[64] A. Bartler, L. Mauch, B. Yang, M. Reuter, and L. Stoicescu, "Automated detection of solar cell defects with deep learning," in 2018 26th European signal processing conference (EUSIPCO), 2018, pp. 2035–2039. DOI: https://doi.org/10.23919/EUSIPCO.2018.8553025

[65] S. Deitsch et al., "Automatic classification of defective photovoltaic module cells in electroluminescence images," Sol. Energy, vol. 185, pp. 455–468, 2019. DOI: https://doi.org/10.1016/j.solener.2019.02.067

[66] B. Ni, P. Zou, Q. Li, and Y. Chen, "Intelligent defect detection method of photovoltaic modules based on deep learning," vol, vol. 161, pp. 167–173, 2018. DOI: https://doi.org/10.2991/tlicsc-18.2018.27

[67] M. R. U. Rahman and H. Chen, "Defects inspection in polycrystalline solar cells electroluminescence images using deep learning," IEEE Access, vol. 8, pp. 40547–40558, 2020. DOI: https://doi.org/10.1109/ACCESS.2020.2976843

[68] J. Wang, B. Zhao, and X. Yao, "PV Abnormal Shading Detection Based on Convolutional Neural Network," in 2020 Chinese Control And Decision Conference (CCDC), 2020, pp. 1580–1583. DOI: https://doi.org/10.1109/CCDC49329.2020.9164630

[69] B. Du, Y. He, Y. He, J. Duan, and Y. Zhang, "Intelligent classification of silicon photovoltaic cell defects based on eddy current thermography and convolution neural network," IEEE Trans. Ind. Informatics, vol. 16, no. 10, pp. 6242–6251, 2019. DOI: https://doi.org/10.1109/TII.2019.2952261

[70] J. Balzategui et al., "Semi-automatic quality inspection of solar cell based on Convolutional Neural Networks," in 2019 24th IEEE International Conference on Emerging Technologies and Factory Automation (ETFA), 2019, pp. 529–535. DOI: https://doi.org/10.1109/ETFA.2019.8869359

[71] Y. Tan, K. Liao, X. Bai, C. Deng, Z. Zhao, and B. Zhao, "Denoising Convolutional Neural Networks Based Dust Accumulation Status Evaluation of Photovoltaic Panel," in 2019 IEEE International Conference on Energy Internet (ICEI), 2019, pp. 560–566. DOI: https://doi.org/10.1109/ICEI.2019.00105

[72] X. Li, Q. Yang, J. Wang, Z. Chen, and W. Yan, "Intelligent fault pattern recognition of aerial photovoltaic module images based on deep learning technique," J. Syst. Cybern. Inf, vol. 16, pp. 67–71, 2018. DOI: Not available.

[73] X. Li, W. Li, Q. Yang, W. Yan, and A. Y. Zomaya, "Building an online defect detection system for large-scale photovoltaic plants," in Proceedings of the 6th ACM International Conference on Systems for Energy-Efficient Buildings, Cities, and Transportation, 2019, pp. 253–262. DOI: https://doi.org/10.1145/3360322.3360835

[74] X. Qian, J. Li, J. Cao, Y. Wu, and W. Wang, “Micro-cracks detection of solar cells surface via combining short-term and long-term deep features,” Neural Networks, vol. 127, pp. 132–140, 2020. DOI: https://doi.org/10.1016/j.neunet.2020.04.012

[75] M. Manohar, E. Koley, and S. Ghosh, “Enhancing the reliability of protection scheme for PV integrated microgrid by discriminating between array faults and symmetrical line faults using sparse auto encoder,” IET Renew. Power Gener., vol. 13, no. 2, pp. 308–317, 2019. DOI: https://doi.org/10.1049/iet-rpg.2018.5627

[76] X. Lu et al., “Fault diagnosis for photovoltaic array based on convolutional neural network and electrical time series graph,” Energy Convers. Manag., vol. 196, pp. 950–965, 2019. DOI: https://doi.org/10.1016/j.enconman.2019.06.062

[77] Z. Chen, Y. Chen, L. Wu, S. Cheng, and P. Lin, “Deep residual network based fault detection and diagnosis of photovoltaic arrays using current-voltage curves and ambient conditions,” Energy Convers. Manag., vol. 198, p. 111793, 2019. DOI: https://doi.org/10.1016/j.enconman.2019.111793

[78] W. Gao and R.-J. Wai, “A novel fault identification method for photovoltaic array via convolutional neural network and residual gated recurrent unit,” IEEE access, vol. 8, pp. 159493–159510, 2020. DOI: https://doi.org/10.1109/ACCESS.2020.3020296

[79] M. W. Hopwood, T. Gunda, H. Seigneur, and J. Walters, “Neural network-based classification of string-level IV curves from physically-induced failures of photovoltaic modules,” IEEE Access, vol. 8, pp. 161480–161487, 2020. DOI: https://doi.org/10.1109/ACCESS.2020.3021577

[80] X. Li, Q. Yang, Z. Lou, and W. Yan, “Deep learning based module defect analysis for large-scale photovoltaic farms,” IEEE Trans. Energy Convers., vol. 34, no. 1, pp. 520–529, 2018. DOI: https://doi.org/10.1109/TEC.2018.2873358

[81] A. Y. Appiah, X. Zhang, B. B. K. Ayawli, and F. Kyeremeh, “Long short-Term memory networks based automatic feature extraction for photovoltaic array fault diagnosis,” IEEE Access, vol. 7. pp. 30089–30101, 2019. DOI: https://doi.org/10.1109/ACCESS.2019.2902949

[82] X. Lu et al., “Fault diagnosis model for photovoltaic array using a dual-channels convolutional neural network with a feature selection structure,” Energy Convers. Manag., vol. 248, p. 114777, 2021. DOI: https://doi.org/10.1016/j.enconman.2021.114777

[83] F. Hong, J. Song, H. Meng, R. Wang, F. Fang, and G. Zhang, “A novel framework on intelligent detection for module defects of PV plant combining the visible and infrared images,” Sol. Energy, vol. 236, pp. 406–416, 2022. DOI: https://doi.org/10.1016/j.solener.2022.03.018

[84] K. Ishaque, Z. Salam, and H. Taheri, “Accurate MATLAB simulink PV system simulator based on a two-diode model,” J. power Electron., vol. 11, no. 2, pp. 179–187, 2011. DOI: https://doi.org/10.6113/JPE.2011.11.2.179

[85] C. L. Nkashama, “Maximum power point tracking algorithm for photovoltaic home power supply.” 2011. DOI: Not available.

[86] A. Krizhevsky, I. Sutskever, and G. E. Hinton, “Imagenet classification with deep convolutional neural networks,” Adv. Neural Inf. Process. Syst., vol. 25, 2012. DOI (later reprint): https://doi.org/10.1145/3065386

[87] A Saifoddin, M Kalantari and M Allahrabbi Shirazi, "Comparison and Review of the Application of Deep Learning Models in Forecasting Electrical Energy Generation of Photovoltaic Systems with a Focus on LSTM and Hybrid Models," Science and Technology in Mechanical Engineering, (2026): e242944. DOI: Not yet verified.

[88] Allahrabbi Shirazi, Mohammad Ali, Ali Goldoust, Mohanna Khatami, Erfan Abedi, and Mohammad Hassan Janfeshan. "Modeling and simulation of a solar tracker with bifacial panel: a case study of Tehran city." Journal of Sustainable Energy Systems 3, no. 3 (2024): 271-287. DOI: https://doi.org/10.22059/ses.2024.379035.1078

[89] Saifoddin, Amirali, Negin Mirzaei, Mohammadali Allahrabbi Shirazi, and Hossein Yousefi. "Comparative Applications of Supervised and Unsupervised Machine Learning Models in Energy Systems." Journal of Energy Management and Technology 9, no. 4 (2025): 284-290. DOI: https://doi.org/10.22109/jemt.2025.547118.1573